Normal Grain Growth: Monte Carlo Potts Model Simulation and Mean-Field Theory

D. Zöllner and P. Streitenberger

Institut für Experimentelle Physik, Otto-von-Guericke-Universität Magdeburg

Abstract. Grain growth in polycrystals is modelled using an improved Monte Carlo Potts model algorithm. By extensive simulation of three-dimensional normal grain growth it is shown that the simulated microstructure reaches a quasi-stationary self-similar coarsening state, where especially the growth of grains can be described by an average self-similar growth law, which depends only on the number of faces described by a square-root law. Together with topological considerations a non-linear effective growth law results. A generalized analytic mean-field theory based on the growth law yields a scaled grain size distribution function that is in excellent agreement with the simulation results. Additionally, a comparison of simulation and theory with experimental results is performed.

1 Introduction

Many technical properties of polycrystalline materials depend strongly on the grain size of the microstructure. The control of the microstructure is a key to improve material's properties like, e.g., strength, toughness, diffusivity and electrical conductivity in processing. On the other hand, many technical processes lead, e.g., by thermal influence, to grain growth, which is the migration of a grain boundary driven by the boundary energy. The associated thermodynamic driving force is the decrease in the Gibbs free interface energy. In this process the mean grain size increases with a simultaneous decrease of the total inner interface leading to a minimization of the total interface free energy. In order to study the phenomenon of grain growth more closely, first physically motivated grain growth models have been developed in the early 1950s (Smith 1952; Burke and Turnbull 1952). However, there remained clear discrepancies between the theories and experiments.

A new approach has been provided in the 1980s by computer simulations as new possibilities to model the grain microstructure and its temporal evolution under realistic conditions allowing for the observation of features that are difficult to observe experimentally, like, e.g., the surface or the rate of volume change of individual grains. Due to the broad field of applicability a number of different simulation methods have been developed throughout the years like, e.g., the Monte Carlo Potts model, the phase-field method, the Surface Evolver, and the vertex method (compare, e.g., (Miodownik 2002; Atkinson 1988; Thompson 2001)).

Among the above methods, the Monte Carlo Potts model is the most widely used one. The model is in its basics simple but in its specifics rather complex and therewith flexible. Hence, it can be applied efficiently to complex microstructures. Within the

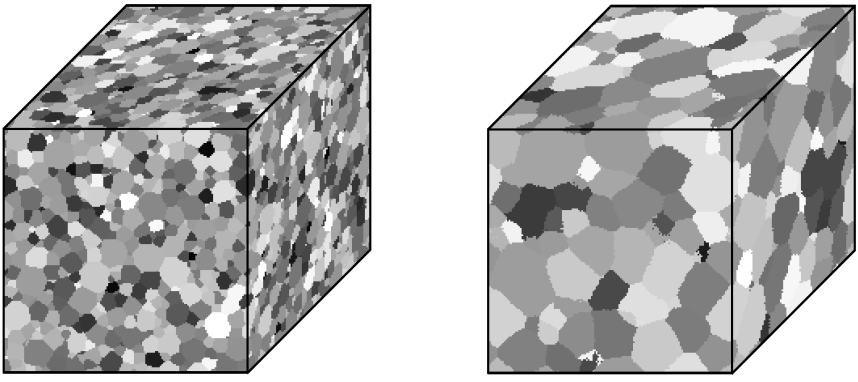

Fig. 1. Simulated 3D grain structures at different grain growth stages

scope of the authors present work the Monte Carlo Potts model method has been implemented in two and three dimensions based on the original works of (Anderson et al. 1984; Srolovitz et al. 1984; Anderson et al. 1989) including improvements in the algorithm, which have been suggested recently (e.g., (Yu and Esche 2003; Kim et al. 2005; Zöllner 2006) and the references within).

2 Monte Carlo Potts Model Simulation

Before a simulation can be started, the continuously given microstructure has to be mapped onto a discrete lattice. In three dimensions a cubic lattice is usually used with 26 nearest neighbours (first, second, and third nearest neighbours). Although the cubic 3D resp. quadratic 2D lattice is the simplest one for implementation, there has been a discussion throughout the years, whether this underlying lattice constrains the simulation results. In Figure 2 one can see that the grain boundaries cling to the underlying lattice. The reason for this effect is substantiated in the Potts model itself as the driving force places the boundaries along the lattice facets yielding a growth kinetics that differs from the expected normal grain growth (Holm et al. 1991 and 2001).

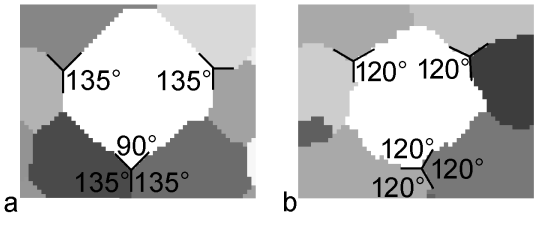

Fig. 2. a – clinging of the grain boundaries to the lattice at zero simulation temperature; b – grain boundaries with 120° angles at high simulation temperatures

Since these lattice effects depend strictly on the simulation algorithm and are highly non-physical, one has to eliminate them, e.g., following (Holm et al. 1991) by increasing the defined number of neighbouring lattice points or the simulation temperature T activating thermal fluctuations. In Figure 2b one can see that independent of the underlying lattice the angles adjust at 120° in the triple points for a non-zero temperature.

Each lattice point represents in the simulation a Monte Carlo unit (MCU), to which a crystallographic orientation is assigned specified by the rotation angles in the three-dimensional Euler space. The rotation angles specify the relative orientation to the given fixed coordinate system of the lattice (Ivasishin et al. 2003). In the simulation the orientation is usually represented by natural numbers.

The smallest time unit of the Monte Carlo Potts model simulation is called a Monte Carlo step (MCS) and defined as N reorientation attempts, where N is equal to the total number of MCUs, i.e., lattice points of the lattice.

The basic Potts algorithm (Anderson et al. 1984 and 1989; Srolovitz et al. 1984) shows some disadvantages that are inherent to the technique, e.g., unrealistic nucleation events and a growth exponent in Eq. (1) smaller than the expected value of $n = 0.5$. Furthermore, the basic algorithm is very time consuming. Especially in recent times, changes in the algorithm have been suggested improving the accuracy of the simulation results and reducing the runtime of the simulations (Yu and Esche 2003; Zöllner and Streitenberger 2004; Kim et al. 2005; Zöllner 2006).

Each of the N reorientation attempts consists of the following steps.

In the first step a MCU is chosen in a probabilistic way. This MCU has an orientation Q_μ (old state). But mostly the chosen MCU will be inside a grain and not on a boundary. Hence, unrealistic nucleation events may occur due to fluctuations induced by the simulation temperature. Seeing that grain growth always means grain boundary migration, a change of orientation can only occur if the chosen MCU is on the boundary. In this case the simulation algorithm proceeds with Step 2, otherwise the algorithm terminates this loop (Step 1).

In the second step a new orientation Q_ν different from the old orientation Q_μ is assigned on probation to the chosen MCU. This new orientation is chosen from all other (Q-1) orientations, where Q is the total number of orientations. However, most reorientation attempts will fail or again unrealistic nucleation events happen. Therefore, only orientations of the neighbouring MCUs are considered, because of the above grain boundary migration argument.

In the third step the energy of both states is given by the Hamiltonian

$$H = J \cdot \sum_{i=1}^{N} \sum_{j=1}^{nn} \left(1 - \delta_{Q_i Q_j}\right).$$

The inner sum sums up over the nearest neighbours of the i-th MCU and the outer sum over all N MCUs of the lattice. Due to the Kronecker delta each pair of nearest neighbours contributes J to the system energy, if they do not have the same orientation, and 0 otherwise, where J measures the interaction of the i-th MCU with all neighbouring MCUs as a function of the misorientation angle θ between two grains calculated by the Read-Shockley equation (Read and Shockley 1950)

$$J = \begin{cases} \dfrac{\theta}{\theta^*} \cdot \left(1 - \ln \dfrac{\theta}{\theta^*}\right), & \text{if } \theta \le \theta^* \\ 1, & \text{if } \theta \le \theta^* \end{cases},$$

where θ^* is the maximal value of a low angle grain boundary. From experiments it is known to be between 10° and 30° depending on the material (Sutton and Balluffi 1995) (compare also (Read and Shockley 1950; Hui et al. 2003) and the literature therein). For simulations of normal grain growth, where only high angle grain boundaries occur, it holds $J = 1$ (Fig. 3b).

In the fourth step the difference in energy ΔE between new and old state is calculated. However, due to the fact that from the whole lattice only one MCU is reoriented at a time, the difference in energy can simply be calculated as

$$\Delta E = J \cdot \sum_{j=1}^{nn} \left(\delta_{Q_j Q_\mu} - \delta_{Q_j Q_\nu}\right).$$

Finally – in the fifth step – the final state with the final orientation Q_μ^* of the selected MCU is chosen with the probability p given by

$$p = \begin{cases} m, & \Delta E \le 0 \\ m \cdot \exp \dfrac{-\Delta E}{k_B T}, & \Delta E > 0 \end{cases},$$

where k_B is Boltzmann's constant and T the simulation temperature (Fig. 3a).

It should be mentioned here again that the factor T does not measure a real temperature but rather represents a parameter of the probability-jump-function introduced to avoid lattice pinning.

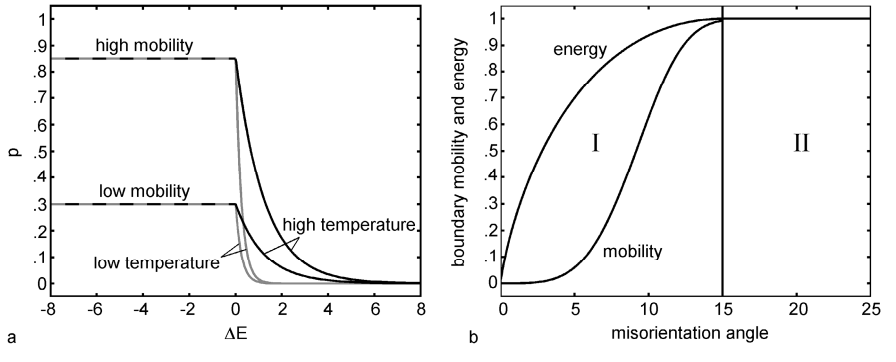

Fig. 3. a – Probability p for acceptance of orientation; b – boundary mobility and energy depending on misorientation angle

The boundary mobility is also a function of the misorientation angle (Fig. 3b)

$$m = \begin{cases} 1 - \exp\left(-B \cdot \left(\dfrac{\theta}{\theta^*} \right)^n \right), & \text{if } \theta \le \theta^* \\ 1, & \text{if } \theta > \theta^* \end{cases}$$

given by (Huang and Humphreys 2000). The constants are $B = 5$ and $n = 4$.

3 Monte Carlo Simulation Results

The coarsening process has been investigated by following the temporal development of 3D grain microstructures simulated by the Monte Carlo Potts model simulation. These microstructures are initially either Rayleigh distributed structures or Voronoi Tessellations (Zöllner 2006).

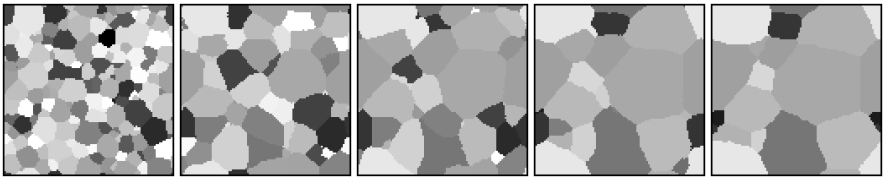

Fig. 4. 3D coarsening process shown through temporal development of a 2D section

The size of the lattice has been chosen as 200×200×200 with periodic boundary conditions and the simulation temperature is $k_BT = 2.6$. For analyses the simulation results are averaged for each simulation step over ten simulation runs.

3.1 Coarsening Process: Growth Law, Scaling Regime and Grain Size Distribution

Curvature-driven normal grain growth – as simulated by the Monte Carlo Potts model – can essentially be characterized by a parabolic growth law and statistical self-similarity (cf. the review articles (Atkinson 1988; Thompson 2001)).

The average grain size $\langle R \rangle$ of an ensemble of grains of a polycrystalline solid increases with time t according to the parabolic growth law

$$\langle R \rangle^n - \langle R \rangle_0^n = b \cdot t \,, \tag{1}$$

where R is the radius of a grain volume equivalent sphere, b is the growth factor and n is the growth exponent, which is theoretically supposed to be 0.5. The volume of each grain is equal to the number of MCUs representing the grain.

Both 3D grain structures as they have been simulated (Zöllner and Streitenberger 2008) by the Monte Carlo Potts model follow after an initial period of time (Figure 5a and b, part I) the well-known growth law, Eq. (1), (Figure 5a and b, part II). For both structures the numerically given growth exponent n is in very good agreement with

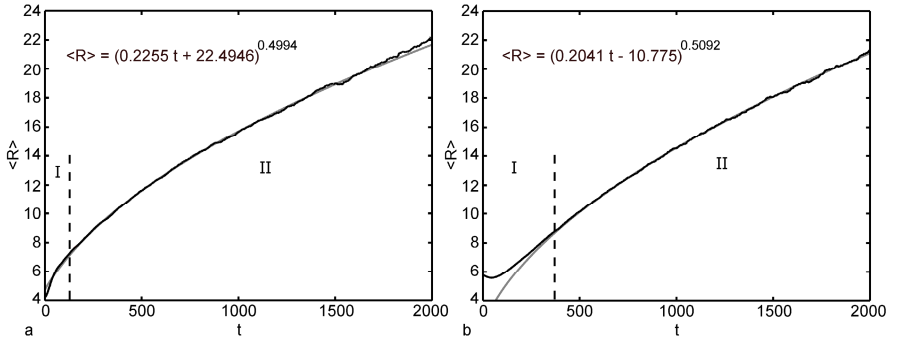

Fig. 5. Temporal development of the mean grain size (black) with initial period (I) and self-similar coarsening regime (II) together with fit (grey) of growth law, Eq. (1): a – for the Rayleigh distributed grain ensemble; b – for the Voronoi tessellated grain ensemble

the expected value of $n = 0.5$ in Eq. (1), which can be found in all three fields of investigation of normal grain growth, namely experiments, theory and computer simulations (compare (Yu and Esche 2003)).

The initially Rayleigh distributed grain ensemble reaches faster than the initial Voronoi tessellation the state characterised by the growth law, Eq. (1). The authors have shown (cf. Fig. 3b in (Zöllner and Streitenberger 2008)) that the number of grains reaching this state is significant larger for the initially Rayleigh distributed structure (approx. 34% grains left) than for the initial Voronoi structure (with approx. 20% grains left). Therefore, the initially Rayleigh distributed grain structure is used for further statistical analyses.

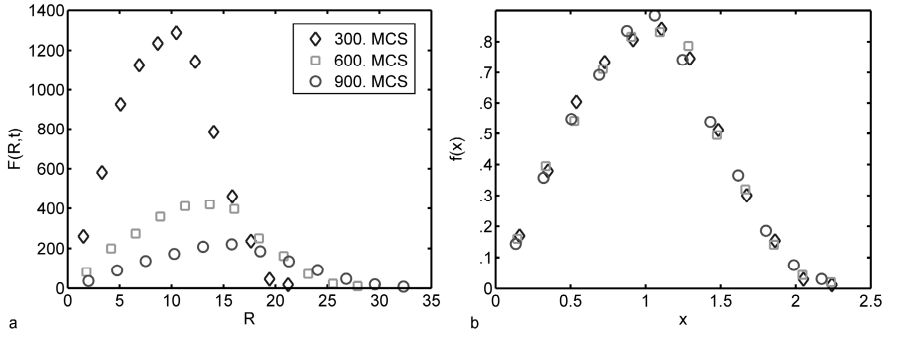

Fig. 6. a – Absolute grain size distribution showing number of grains vs. grain size; b - relative size distribution with relative number of grains vs. relative grain size $x = R/\langle R \rangle$

Contemporary, the coarsening process of the grain structure develops towards a quasi-stationary state that exhibits statistical self-similarity (Burke 1949; Mullins 1986). The grain size distribution function $F(R,t)$ in the quasi-stationary state is characterized by the scaling form

$$F(R,t) = g(t) \cdot f(x), \; x = \frac{R}{\langle R \rangle}. \tag{2}$$

All scaled grain size distribution functions $f(x)$ within this quasi-stationary self-similar coarsening regime collapse to a single universal, time-independent size distribution as shown in Figure 6b, where three time steps out of the quasi-stationary self-similar state indeed coincide. The temporal development of the size distribution can be seen best by looking at the absolute size distribution in Figure 6a (compare (Zöllner 2006; Zöllner and Streitenberger 2006, 2007b and 2008)).

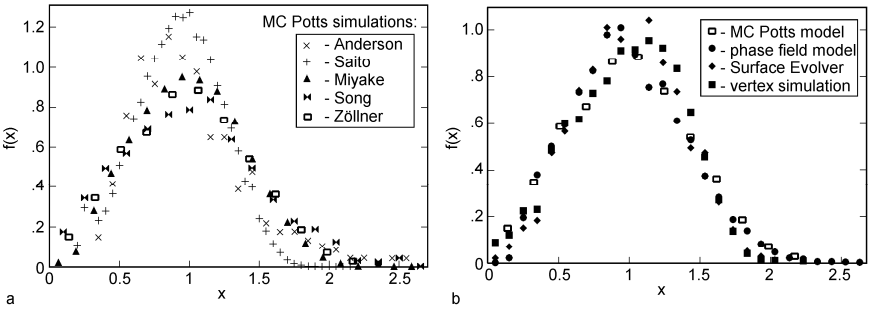

Fig. 7. Comparison of the simulated grain size distribution with the results of: a – other Monte Carlo Potts model simulations; b – other simulation methods both taken from literature (Krill and Chen 2002)

Figure 7a shows the simulated self-similar grain size distribution within the quasi-stationary coarsening regime in comparison to Monte Carlo Potts model simulations of (Anderson et al. 1989; Saito 1998; Miyake 1998; Song and Liu 1998), which have been taken from (Krill and Chen 2002). The grain size distribution of the simulation of the authors (blank squares) is very similar to that of other simulations. Deviations can be explained by the use of different simulation parameters like, e.g., simulation temperature or underlying lattice.

The comparison between the grain size distribution obtained in this work with results of other simulation methods, namely the phase-field simulation of (Krill and Chen 2002), the Surface Evolver approach of (Wakai et al. 2000) and the vertex method of (Weygand et al. 1999), shows an even better agreement (Figure 7b).

3.2 Topology: Number of Faces vs. Grain Size

The correlation between the number of faces s per grain and the relative grain size x is an important topological feature of the microstructure. Due to the relaxation process connected with grain growth this correlation changes with time. However, it is known that the average number of faces of a grain of given size can be described within the quasi-stationary self-similar state by a time-invariant function of the relative grain size x (cf. Fig. 8b).

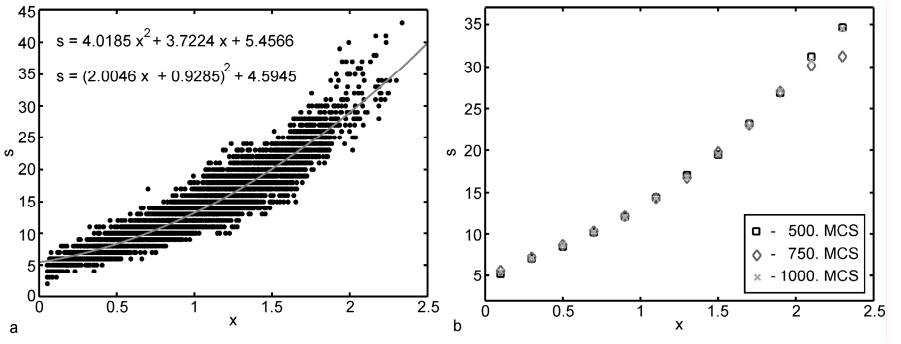

Fig. 8. a – Number of faces vs. relative grain size for all grains of an ensemble for the 500th MCS together with quadratic least-squares fit; b – average number of faces vs. relative grain size divided into size classes for three different time steps

Within the quasi-stationary state the number of faces of the individual grains depends non-linearly on the relative grain size (compare Fig. 8a). The relation can be approximated in the average by a non-binomial parabolic function

$$s(x) = s_2 x^2 + s_1 x + s_0 = (px+q)^2 + \delta\,. \tag{3}$$

This is consistent with experimental observations (Zhang et al. 2004), geometrical considerations following (Abbruzzese and Lücke 1996; Streitenberger and Zöllner 2006; Zöllner 2006) and 3D computer simulations (Wakai et al. 2000).

3.3 Volumetric Rate of Change

In the quasi-stationary state the growth of each grain can be described by the average self-similar growth law (Streitenberger 1998; Streitenberger and Zöllner 2006 and 2007)

$$\dot{R} = \frac{dR}{dt} = \frac{k}{R}\cdot H(x). \tag{4}$$

$H(x)$ is a time-invariant dimensionless function of the relative grain size, and k is the kinetic constant of curvature driven grain boundary motion. According to this equation $R\dot{R}$ is directly linked to the volume change rate with

$$V^{-1/3}\dot{V} = \zeta\cdot R\dot{R} = k\cdot\zeta\cdot H(x);\quad \zeta = \left(48\pi^2\right)^{1/3} \tag{5}$$

In recent times, (Hilgenfeldt et. al. 2001) and (Glicksman 2005) have shown by considering three-dimensional space filling polyhedral networks that the average volumetric rate of change is solely a function of its average number of faces or neighbours $s = s(x)$ and can be approximated by the expression

$$R\dot{R} = C_0 + C_1\sqrt{s}\,, \tag{6}$$

which can be considered as the 3D analogue to the von Neumann–Mullins law.

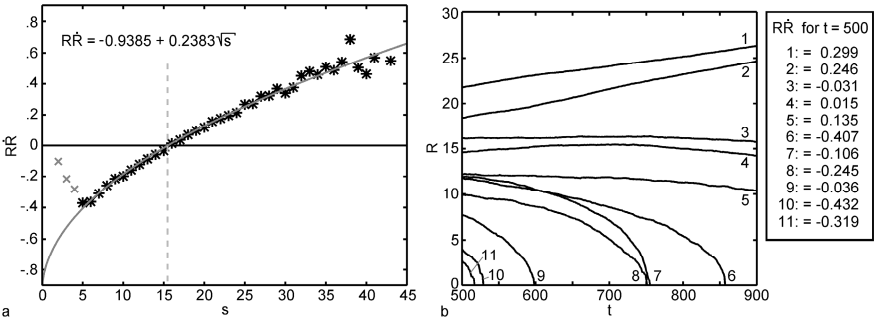

Fig. 9. a – Volumetric rate of change vs. number of faces for 500th MCS with fit of Eq. (6); b – development of grain size for some selected grains together with volume change rate

Figure 9a shows $R\dot{R}$ vs. s as it follows from the Monte Carlo simulation, where $\dot{R} \approx \Delta R / \Delta t$ is approximated (Zöllner and Streitenberger 2004 and 2006). The least-square fit of Eq. (6) to the simulation data yields a very good representation. Deviations for small grains are inherent to the simulation technique. It can be seen that the fitted values C_0 = -0.9385 and C_1 = 0.23829 are close to Glicksman's theoretical values $C_{0\,\mathrm{Glicksman}}$ = -1.0583 and $C_{1\,\mathrm{Glicksman}}$ = 0.2886 (normalized by $1/\zeta$ as it is given in Eq. (5)).

Additionally, in Figure 9b it is shown that in general grains with a volumetric rate of change larger than zero grow (curves 1 and 2), nearly equal to zero do not change (curves 3, 4 and 5) and smaller than zero shrink (curves 6 to 11) (compare also (Zöllner and Streitenberger 2007a).

In Figure 10a it appears that the simulated volumetric rate of change can be approximated by a quadratic polynomial in x (Zöllner and Streitenberger 2007b)

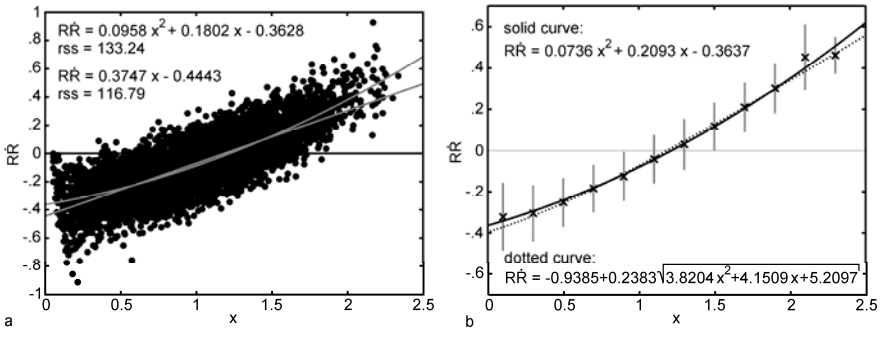

Fig. 10. a – Self-similar volumetric rate of change vs. relative grain size for all simulation data together with linear and quadratic least-squares fits; b - self-similar volumetric rate of change vs. relative grain size for data divided into size classes together with fit of Eq. (7) (solid curve) and plot of Eq. (6) with $s(x)$ from Eq. (3) as they both follow from fits to simulation data (dotted curve).

$$R\dot{R} = kH(x) = a_2 x^2 + a_1 x + a_0 . \tag{7}$$

This is consistent with the non-linear behaviour of the effective growth law resulting from the combination of Eqs. (3) and (6), which leads to an effective growth law in the form of Eq. (4), where contrary to Hillert's assumption $H(x)$ is a non-linear function, (Figure 10b).

4 Mean-Field Theory

In the statistical mean-field theory of grain growth [Zöllner (2006)] it is assumed that the growth of grains can be described by an average self-similar growth law, Eq. (4), for all grains of size R so that the grain size distribution function $F(R,t)$, characterized by the scaling form, Eq. (2), obeys the continuity equation

$$\frac{\partial F(R,t)}{\partial t} + \frac{\partial}{\partial R}\left(\dot{R}F(R,t)\right) = 0 . \tag{8}$$

In his pioneering work on grain growth (Hillert 1965) assumed a linear function for $H(x)$. Using stability arguments of the coarsening theory of (Lifshitz and Slyozov 1961; Wagner 1961) Hillert obtained his well-known grain size distribution function (Hillert 1965), which, however, never has been observed, neither experimentally nor by computer simulations.

Based on the parabolic approximation, Eq. (7), and the scaling assumption (2) for the grain size distribution, the integration of the continuity equation yields the following analytical expression for the normalized scaled grain size distribution function (Streitenberger and Zöllner 2006; Zöllner 2006),

$$f(x) = \frac{1}{x_c}\varphi\left(\frac{x}{x_c}\right), \tag{9}$$

$$\begin{aligned}
&\varphi(u) = \frac{D[\gamma+\alpha\gamma]^{D/[2(1-\alpha\gamma)]}u}{\left[(1-\alpha\gamma)u^2 - \gamma u + \gamma + \alpha\gamma\right]^{1+D/[2(1-\alpha\gamma)]}} * \\
&\exp\left\{\frac{-D\gamma}{(1-\alpha\gamma)\sqrt{\Delta}}\left[\arctan\frac{-\gamma+2(1-\alpha\gamma)u}{\sqrt{\Delta}} - \arctan\frac{-\gamma}{\sqrt{\Delta}}\right]\right\} \\
&x_c = 1/\int u\varphi(u)du \\
&\Delta = 4\gamma(1+\alpha)(1-\alpha\gamma) - \gamma^2 \geq 0.
\end{aligned} \tag{10}$$

Eq. (10) represents a two-parameter family of grain size distribution functions (Fig. 11a), which fulfil the requirement of volume conservation in conjunction with the existence of the D-th moment $\langle u^D \rangle$ of the grain size distribution function if the parameters α and γ obey the conditions (Streitenberger and Zöllner 2006)

$$\begin{aligned}
&\gamma \leq \frac{4(1+\alpha)}{4\alpha(1+\alpha)+1}, && \text{if } \alpha > 0 \\
&\gamma = 4, && \text{if } \alpha = 0
\end{aligned} . \tag{11}$$

For the limiting case $\Delta = 0$, that is for $4\gamma(1+\alpha)(1-\alpha\gamma)-\gamma^2 = 0$, Eq. (10) reduces to the one-parameter function (Fig. 11b)

$$\varphi(u) = \begin{cases} a \cdot u_0^{\,a} \cdot \exp(a) \cdot \dfrac{u}{(u_0 - u)^{a+2}} \exp\left(-\dfrac{a \cdot u_0}{u_0 - u}\right), & 0 \le u \le u_0 \\ 0, & \text{otherwise} \end{cases}, \qquad (12)$$

with $a = D(u_0 - 1)^2$, showing a finite cut-off at u_0 considered already in (Streitenberger 1998 and 2001, Zöllner and Streitenberger 2004 and 2006).

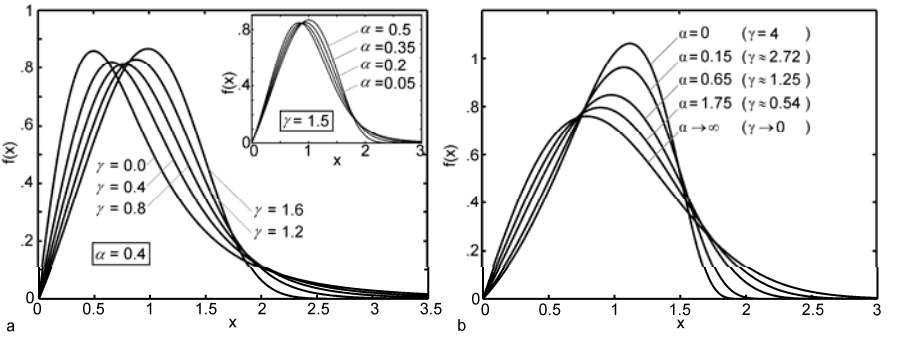

Fig. 11. Analytic grain size distribution functions: a – Eq. (10) rescaled to $f(x)$ for D = 3 and $\Delta > 0$; b – Eq. (12) for D = 3 and $\Delta = 0$.

5 Comparison of Simulation with Experimental Measurements and Analytical Theory

It is a well known problem that sections through a 3D grain ensemble yield smaller 2D grain sizes than the real 3D grain sizes (Ohser and Mücklich 2000). Parallel sections through grains yield different sizes and forms depending on place and orientation of the sectioning (compare Fig. 12).

Since most experimentally determined size distributions come from sectioning (Ohser and Mücklich 2000), for comparison 2D sections of the simulated 3D microstructure have to be used. In this case (Fig. 13a) experimental data of zone-refined iron, which shows normal grain growth, have been used determined by (Hu 1974). Despite some minor differences there is a good overall agreement between the 2D sectioning data from experiment and simulation (Zöllner and Strei-tenberger 2007c).

The comparison of 3D grain size distributions from simulation with experimental results for recrystallized and annealed pure polycrystalline iron obtained by serial sectioning (Zhang et al. 2004) is shown in Figure 13b, where additionally a fit of the theoretical expression Eq. (10) to our simulation data is plotted. It can be seen that the experimental size distribution of Zhang et al. shows some differences (Zöllner and Streitenberger 2007c). The reason why it is more peaked is unclear.

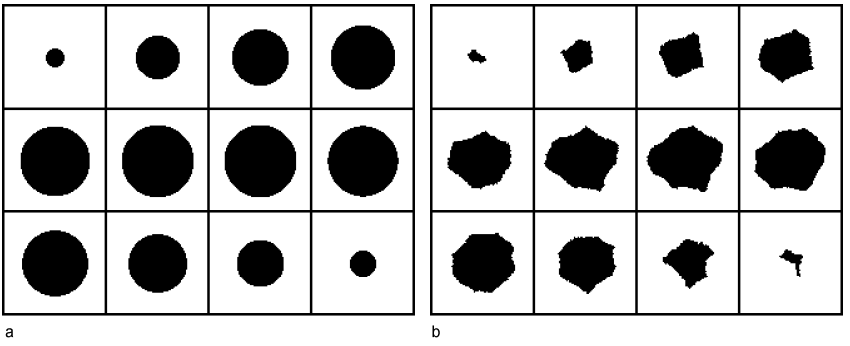

Fig. 12. Equally distanced sections through: a – a sphere; b – a grain

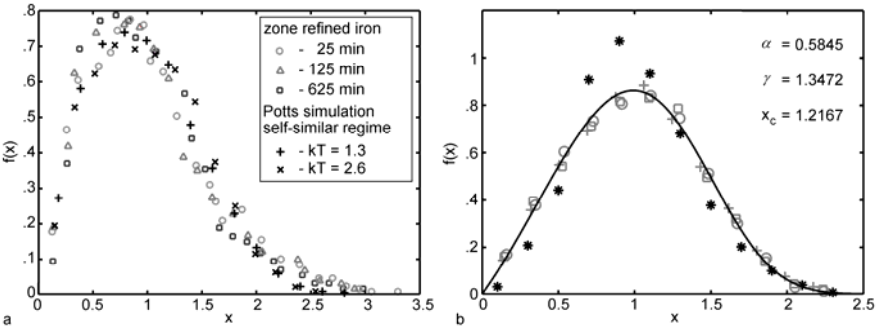

Fig. 13. Relative grain size distributions: a – of experimental data (Hu 1974) compared to 2D sections from Monte Carlo simulation; b – from experimental data (black stars) obtained by serial sectioning (Zhang et al. 2004) compared to simulated self-similar 3D size distribution (grey) with analytical fit, Eq. (10)

The least-squares fits of eqs. (10) and (12) to the simulation data are in very good agreement with the simulation results (Figure 14a). It can rather be seen that the one-parameter function is an approximation as good as the two parameter one.

The parameters α and γ can also be determined (Streitenberger and Zöllner 2006) from the parameters of the quadratic average growth law (7) fitted to the simulated microstructure (Fig. 10a). While α can be calculated immediately from $\alpha = a_2 x_c / a_1 = 0.6492$, γ is determined self-consistently by the scaling requirement that the scaled critical grain size $x_c = 1.22309$ of the simulated microstructure following from $\dot{R}(x_c) = 0$ has to be the same as $x_c = 1/\int u\varphi(u)du$ following from the grain size distribution function, (10), yielding $\gamma = 1.24876$. The resulting analytical grain size distribution function is in excellent agreement with the grain size distribution of the Monte Carlo Potts model simulation as shown in Figure 14b.

A comparison of the least-squares fit of Eq. (10) to the simulated size distribution with the analytical size distribution functions of (Hillert 1965) and (Louat 1974) are

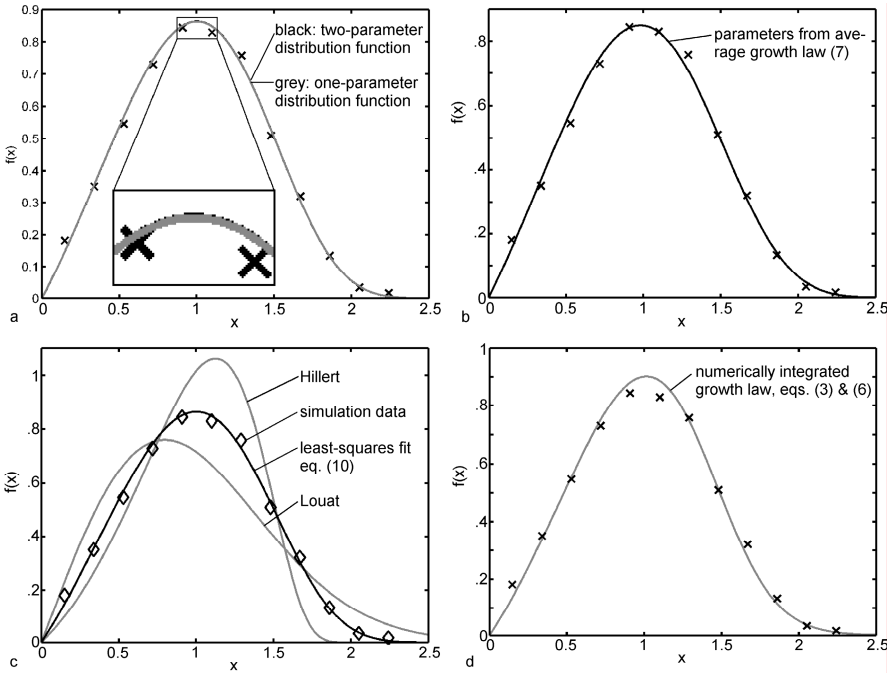

Fig. 14. Simulated grain size distribution together with: a – least-squares fit of (10) and (12); b – fit of (10) with parameters given by average growth law, Eq. (7); c – least-squares fit of (10), Hillerts (Eq. (10) for $\alpha = 0$) and Louats (Eq. (10) for $\alpha \to \infty$) size distribution; d – size distribution obtained by integration of average growth law (6) with Eq. (3).

shown in Figure 14c, where it is clear that the simulated distribution can be approximated very well by our theory but is quite different from the distributions of Hillert and Louat.

The average growth law $R\dot{R}$ can also be used free of the parabolic approximation, Eq. (7). Therefore, the non-linear growth law (6) is used as it has been fitted to the simulation results in Figure 9a. The function $s(x)$ is given in Figure 8a. Then the grain size distribution results from numerical integration of the growth law and is also in fair agreement with the results as can be seen in Figure 14d.

6 Conclusions

In the present work normal grain growth in three dimensions has been studied on the basis of large-scale Monte Carlo Potts model simulations, which enabled extensive statistical analyses of growth kinetics and topological properties of microstructures within the quasi-stationary coarsening regime. In particular, an average growth law could be derived from the simulation data, involving a quadratic dependency of the self-similar grain-volume change rate on the relative grain size x.

It has been shown that an adequate modification of the effective growth law allows a modification of the Lifshitz-Slyozov-Wagner procedure. Based on the effective growth law derived from simulation data an analytical size distribution function is derived, which is not only fully consistent with the requirement of total-volume conservation and the existence of a finite average grain volume but rather represents the simulation data of three-dimensional grain growth very well.

Additionally, 2D plane sections from simulated 3D grain structures were considered and compared with experimental data showing a very good agreement. The simulated size distribution shows – compared with an experimental grain size distribution for pure iron obtained by serial sectioning – also a fair agreement.

References

Abbruzzese, G., Lücke, K.: Statistical theory of grain growth: a general approach. Mater. Sci. Forum 204-206, 55–70 (1996)

Anderson, M.P., Srolovitz, D.J., Grest, G.S., Sahni, P.S.: Computer simulation of grain growth – 1. Kinetics. Acta Metall. 32, 783–791 (1984)

Anderson, M.P., Grest, G.S., Srolovitz, D.J.: Computer simulation of normal grain growth in three dimensions. Phil. Mag. B 59, 293–329 (1989)

Atkinson, H.V.: Theories of normal grain growth in pure single phase systems. Acta Metall. 36, 469–491 (1988)

Burke, J.E.: Some factor affecting the rate of grain growth in metals. Trans. Metall. Soc. AIME 180, 73–91 (1949)

Burke, J.E., Turnbull, D.: Recrystallization and grain growth. Progr. Met. Phys. 3, 220–292 (1952)

Glicksman, M.E.: Analysis of 3-d network structures. Phil. Mag. 85, 3–31 (2005)

Hilgenfeldt, S., Kraynik, A.M., Koehler, S.A., Stone, H.A.: An accurate von Neumann's law for three-dimensional foams. Phys. Rev. Lett. 86, 2685–2688 (2001)

Hillert, M.: On the theory of normal and abnormal grain growth. Acta Metall. 13, 227–238 (1965)

Holm, E.A., Glazier, J.A., Srolovitz, D., Grest, G.S.: The effect of lattice anisotropy and temperature on domain growth in the two-dimensional Potts model. Phys. Rev. A 43, 2662–2668 (1991)

Holm, E.A., Hassold, G.N., Miodownik, M.A.: On misorientation distribution evolution during anisotropic grain growth. Acta Mater. 49, 2981–2991 (2001)

Hu, H.: Grain growth in zone-refined iron. Can. Metall. 13, 275–286 (1974)

Huang, Y., Humphreys, F.J.: Subgrain growth and low angle boundary mobility in aluminum crystals of orientation {110}<001>. Acta Mater. 48, 2017–2030 (2000)

Hui, L., Guanghou, W., Feng, D., Xiufang, B., Pederiva, F.: Monte Carlo simulation of three-dimensional polycrystalline material. Mater. Sci. Eng. A 357, 153–158 (2003)

Ivasishin, O.M., Shevchenko, S.V., Vasiliev, N.L., Semiatin, S.L.: 3D Monte-Carlo simulation of texture-controlled grain growth. Acta Mater. 51, 1019–1034 (2003)

Kim, Y.J., Hwang, S.K., Kim, M.H., Kwun, S.I., Chae, S.W.: Three-dimensional Monte-Carlo simulation of grain growth using triangular lattice. Mater. Sci. Eng. A 408, 110–120 (2005)

Krill III, C.E., Chen, L.-Q.: Computer simulation of 3-D grain growth using a phase-field model. Acta Mater. 50, 3059–3075 (2002)

Lifshitz, I.M., Slyozov, V.V.: The kinetics of precipitation from supersaturated solid solutions. J. Phys. Chem. Solids 19, 35–50 (1961)

Louat, N.P.: On the theory of normal grain growth. Acta Metall. 22, 721–724 (1974)

Miodownik, M.A.: A review of microstructural computer models used to simulate grain growth and recrystallisation in aluminium alloys. J. Light Metals 2, 125–135 (2002)
Miyake, A.: Monte Carlo simulation of normal grain growth in 2- and 3-dimensions: the lattice-model-independent grain size distribution. Contrib. Mineral. Petrol. 130, 121–133 (1998)
Mullins, W.W.: Two-dimensional motion of idealized grain boundaries. J. Appl. Phys. 27, 900–904 (1956)
Mullins, W.W.: The statistical self-similarity hypothesis in grain growth and particle coarsening. J. Appl. Phys. 59, 1341–1349 (1986)
von Neumann, J.: Written discussion of grain shapes and other metallurgical applications of topology. In: Metal Interfaces, American Society for Metals, Cleveland OH, pp. 108–110 (1952)
Ohser, J., Mücklich, F.: Statistical analysis of microstructures in materials science. Wiley, Chichester (2000)
Read, T.W., Shockley, W.: Dislocation models of crystal grain boundaries. Phys. Rev. 78, 275–289 (1950)
Saito, Y.: Monte Carlo simulation of grain growth in three-dimensions. ISIJ Int. 38, 559–566 (1998)
Smith, C.S.: Grain shapes and other metallurgical applications of topology. In: Metal Interfaces, American Society for Metals, Cleveland OH, pp. 65–109 (1952)
Song, X., Liu, G.: A simple and efficient three-dimensional Monte Carlo simulation of grain growth. Scripta Mater. 38, 1691–1696 (1998)
Srolovitz, D.J., Anderson, M.P., Sahni, P.S., Grest, G.S.: Computer simulation of grain growth – II. Grain size distribution, topology and local dynamics. Acta Metall. 32, 793–802 (1984)
Streitenberger, P.: Generalized Lifshitz-Slyozov theory of grain and particle coarsening for arbitrary cut-off parameter. Scripta Mater. 39, 1719–1724 (1998)
Streitenberger, P.: Analytic model of grain growth based on a generalized LS stability argument and topological relationships. In: Gottstein, G., Molodov, D.A. (eds.) Recrystallization and grain growth, pp. 257–262. Springer, Berlin (2001)
Streitenberger, P., Zöllner, D.: Effective growth law from three-dimensional grain growth simulations and new analytical grain size distribution. Scripta Mater. 55, 461–464 (2006)
Streitenberger, P., Zöllner, D.: Topology based growth law and new analytical grain size distribution function of 3D grain growth. Mater. Sci. Forum 558-559, 1183–1188 (2007)
Sutton, A.P., Balluffi, R.W.: Interfaces in Crystalline Materials. Oxford Science Pub. (1995)
Thompson, C.V.: Grain growth and evolution of other cellular structures. Solid State Phys. 55, 269–316 (2001)
Wagner, C.: Theorie der Alterung von Niederschlägen durch Umlösen (Ostwald-Reifung). Z. Elektrochem. 65, 581–591 (1961)
Wakai, F., Enomoto, N., Ogawa, H.: Three-dimensional microstructural evolution in ideal grain growth - general statistics. Acta Mater. 48, 1297–1311 (2000)
Weygand, D., Bréchet, Y., Lépinoux, J., Gust, W.: Three-dimensional grain growth: A vertex dynamics simulation. Phil. Mag. B 79, 703–716 (1999)
Yu, Q., Esche, S.K.: A Monte Carlo algorithm for single phase normal grain growth with improved accuracy and efficiency. Comp. Mater. Sci. 27, 259–270 (2003)
Zhang, C., Suzuki, A., Ishimaru, T., Enomoto, M.: Characterization of three-dimensional grain structure in polycrystalline iron by serial sectioning. Metall. Mater. Trans. 35A, 1927–1933 (2004)
Zöllner, D.: Monte Carlo Potts Model Simulation and Statistical Mean-Field Theory of Normal Grain Growth. Shaker, Aachen (2006)
Zöllner, D., Streitenberger, P.: Computer Simulations and Statistical Theory of Normal Grain Growth in Two and Three Dimensions. Mater. Sci. Forum 467-470, 1129–1134 (2004)
Zöllner, D., Streitenberger, P.: Three Dimensional Normal Grain Growth: Monte Carlo Potts Model Simulation and Analytical Mean Field Theory. Scripta Mater. 54, 1697–1702 (2006)

Zöllner, D., Streitenberger, P.: Normal Grain Growth in Three Dimensions: Monte Carlo Potts Model Simulation and Mean-Field Theory. Mater. Sci. Forum 550, 589–594 (2007a)
Zöllner, D., Streitenberger, P.: Monte Carlo Potts model simulation and statistical theory of 3D grain growth. Mater. Sci. Forum 558-559, 1219–1224 (2007b)
Zöllner, D., Streitenberger, P.: New analytical grain size distribution in comparison with computer simulated and experimental data. In: Mücklich, F. (ed.) Fortschritte in der Metallographie. Praktische Metallographie Sonderband, vol. 39, pp. 97–102. DGM Werkstoff-Informationsgesellschaft mbH, Frankfurt (2007c)
Zöllner, D., Streitenberger, P.: Monte Carlo Simulation of Normal Grain Growth in Three Dimensions. Mater. Sci. Forum 567-568, 81–84 (2008)